

PAPER • OPEN ACCESS

Numerical assessment of wind turbine blade damage due to contact/impact with tower during installation

To cite this article: Amrit Shankar Verma *et al* 2017 *IOP Conf. Ser.: Mater. Sci. Eng.* **276** 012025

View the [article online](#) for updates and enhancements.

Related content

- [Risk-based approach for rational categorization of damage observations from wind turbine blade inspections](#)
- [Magnus wind turbines as an alternative to the blade ones](#)
- [Numerical Assessment of Ultra-high Performance Concrete Material](#)

Recent citations

- [Effects of Wind-Wave Misalignment on a Wind Turbine Blade Mating Process: Impact Velocities, Blade Root Damages and Structural Safety Assessment](#)
Amrit Shankar Verma *et al*
- [Amrit Shankar Verma *et al*](#)

LIVE AWARDS AND SPECIAL EVENTS

PLenary Lecture:
"Perovskite Solar Cells: Past 10 Years and Next 10 Years" with *Nam-Gyu Park*

Legends of Battery Science:
A Celebration with *M. Stanley Whittingham* and *Akira Yoshino*

PRiME 2020 • October 4-9, 2020
Hosted daily: 2000h ET & 0900h JST/KST

ATTENDEES REGISTER FOR FREE ▶

Numerical assessment of wind turbine blade damage due to contact/impact with tower during installation

^{a,b}**Amrit Shankar Verma***, ^d**Nils Petter Vedvik**, ^{a,b,c}**Zhen Gao**

^aDepartment of Marine Technology, Norwegian University of Science and Technology (NTNU), Trondheim, NO-7491, Norway

^bCentre for Marine Operations in Virtual Environments (SFI MOVE), NTNU, Larsgardsvegen 2, 6009, Ålesund, Norway

^cCentre for Autonomous Marine Operations and Systems (AMOS), NTNU, Trondheim, NO-7491, Norway

^dDepartment of Mechanical and Industrial Engineering, NTNU, Richard Birkelandsvei 2B, NO-7491, Trondheim, Norway

amrit.s.verma@ntnu.no; nils.p.vedvik@ntnu.no; zhen.gao@ntnu.no

*Contact author: amrit.s.verma@ntnu.no

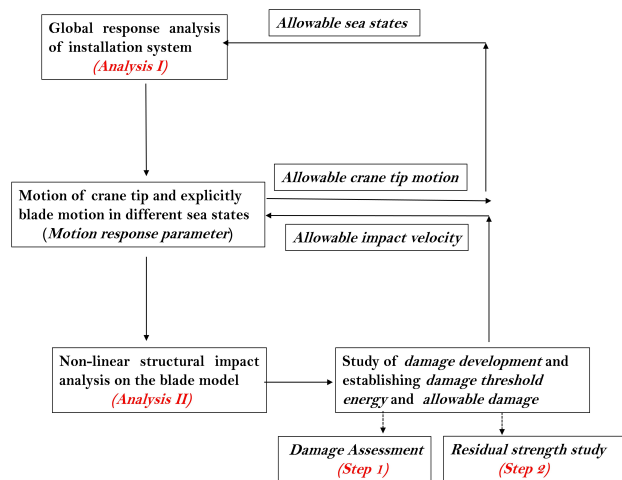
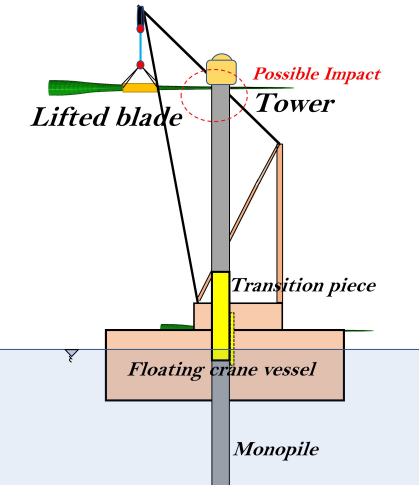
Abstract. The use of floating crane vessel for installation of offshore wind turbine blades presents a great challenge in terms of its random motions and is likely to increase the probability of the blade hitting the preassembled tower during lifting operation. To evaluate the consequences of such scenarios and to determine the allowable motions or sea states for such operations, it is very important to understand the damage development in the blade due to impact. The present paper employs the application of high fidelity finite element method to investigate the damage behavior in the blade when the leading edge of the blade hits the tower. A nonlinear time domain structural analysis using ABAQUS was conducted on the DTU 10 MW reference blade model which is based on shell elements. Damage assessment along with the nature of evolution of various energies is examined and presented for two different impact velocities with modified layup stacking sequence at the contact region.

1. Introduction

The current trend in offshore wind industry is bigger turbines and larger offshore wind farms which demands bigger and heavier components. Moreover, offshore wind industry is developing very fast, moving from shallow water to intermediate water [1]. However, one of the most challenging, risky and cost demanding phases for any offshore wind project is its installation phase [2]. The assembly and installation phase for any offshore wind project is a highly dynamic phase and contributes about 20% of the total CAPEX cost [3, 4]. The contribution of the installation phase to the CAPEX cost is expected to increase in the near future if the current state of the art methods and procedures are used for the planning and execution of marine operations related to offshore wind turbines, most of which are in principle adopted and based on the experiences from traditional oil and gas industry [2]. Thus, the planning and execution of marine operations related to offshore wind farms requires the study of risks and challenges explicitly dedicated to offshore wind turbines, which can further be employed to establish improved and optimized methods and procedures specifically for the installation phases related to the



Content from this work may be used under the terms of the [Creative Commons Attribution 3.0 licence](#). Any further distribution of this work must maintain attribution to the author(s) and the title of the work, journal citation and DOI.

**Figure 1.** Explicit structural response based method**Figure 2.** Illustration showing impact during lifting of the blade using floating crane vessel

offshore wind farms. Such methods should in principle reduce the CAPEX cost by increasing the weather window for installation as well as guarantee the safety of the components and stability of the installation systems by reducing the risk involved in such operations.

One such novel method called explicit response method was proposed by Guachamin Acero, et al. 2016 [3, 5]. This method is based on a very systematic approach that helps in assessment of operational limits for any offshore wind turbine installation operation in general by considering various risks, critical events, limiting response parameters and estimate operational limits [3, 5, 6]. The methodology is based on the numerical simulation of the actual marine operation and operational limits using response based criteria can be derived for a specific marine operation related to offshore wind turbine installation. The details of this generic approach can be found in [3, 5, 6]. In this way, a very practical operational limit can be derived which can be used for planning and execution of marine operation. Guachamin Acero, et al. 2016 [3, 5, 6] has successfully utilized this methodology to estimate the operational limit for mating operation of transition piece with monopile. Li, et al. 2016 [2, 7] has also used this approach to estimate operational limits for initial hammering process of the monopile using the heavy lift floating vessel (HLV). The present paper is motivated towards utilizing and extending this methodology to establish operational limits for the installation phase of a single blade being lifted using a jack up or a floating vessel while considering the risk of impact on the blade and finding damage threshold energy and allowable damage in the blade which will corresponds to allowable impact velocity (motion response parameter) obtained from *Analysis I* to derive back the allowable sea states (Figure 1). This allowable sea state will represent the safe response level for the blade and can be utilized for decision making during real time execution. However, derivation of these limits is out of the scope of this paper and the paper is focused explicitly on the study of damage resistance (*Step 1*) which is the study of damage assessment in the composite structure due to impact [8, 9].

At the moment, mainly jack-up vessels are used for the installations of offshore wind turbines and they provide a very stable platform to carry on operations in the sea but are mostly suitable for shallow water installation works up to the water depth of 30-60 m [5, 10]. However, in the near future, more and more floating installation vessels will be developed and used for installation of offshore wind turbines in intermediate or deep water [1]. The use of floating crane vessel for installation of offshore wind turbines presents great challenges in terms of its random motion mainly induced by wave loads [2, 3, 5, 7] and can lead to impact or contact events during installation owing to their excessive wave induced roll motions and wind and vessel induced crane tip motion (Figure 2). Such an undesirable event can be

quite significant especially for the blades which are composite structures and are very much susceptible to impact induced damages during installation [11].

The sensitivity and the concern for the composite structures to impact induce damage is not new and has been a major concern in the military and aerospace sector. Offshore wind turbine blades are made of composite material as combinations of single skin laminates and sandwich configurations [12] and can also be in principle quite vulnerable to such undesirable impact/contact events when compared with other components made of steel structures getting installed [13, 14]. The property of the anisotropic composite materials is quite complex and has been found very sensitive to both very low and high velocity impact damages as compared to the isotropic steel structures. Steel structures in principle exhibit ductile behavior and the material continue to flow even after yielding in the plastic phase [15] and can dissipate a lot of absorbed energy in the plastic phase before fracture [15]. Composite material on the other hand are brittle in nature and can only dissipate absorbed energy either in the elastic deformation phase or through damage mechanism. These damage mechanisms are susceptible to grow and can cause significant strength reduction due to such impact events [12, 16-21] and thus such damage analysis on the blade is very important if the overall safety level of the installation phase is to be guaranteed. Moreover, the use of sandwich structures further complicates the understanding of blade under impact. There can be other reasons and challenges to do such an analysis on the composite blade. The loads arising due to such impact scenarios on the blade can be very large and questions the integrity of the entire wind turbine blade which are not designed to carry such large impact loads [13, 14]. Again, an offshore wind blade can exhibit several coupled and complex damage and failure modes which can affect the strength of the blade in different ways [22, 23]. The damage on the blade can be in principle localized or distributed [24]. The damage can be failure of fiber in tension (distributed damage), failure of fiber in compression (localized damage), matrix cracking, delamination between the layer of plies in the laminate (interlaminar failure mode), crack through the adhesive joints of trailing edge, leading edge or at the interior bond lines at laminate and beam assembly leading to adhesive failure [24, 25]. It has been shown that delamination of laminates and adhesive bond failure are the most critical damage modes for wind turbine blades [11, 22, 23, 26, 27]. Moreover, the size and location of the delamination also influences the residual compressive strength and reliability in blade [11, 22, 23, 26, 27]. Another challenge for the blade in such impact events is that it is not always feasible to visually inspect such damages, especially damages from small or low velocity impacts and are called barely visible impact damages (BVID) [18, 19, 28]. However, such damages on the blade could still lead to considerable reduction in the strength of the blade and thus it requires a careful study to predict damage mode in the blade under impact to understand the effect of such impact induced damage on the integrity of the blade [18, 19]. Moreover, such damaged blades could demand quite large repair and maintenance cost and could suffer premature failure during its design life if the damage levels are not analyzed and the blades are installed onto the turbine's hub and thus can cause major down time during the productivity hours offshore.

The present paper employs the application of high fidelity finite element method to investigate the damage behavior in the blade when the leading edge of the blade hits the tower. The DTU 10 MW model which is based on shell elements is utilized as the base case for studying such a scenario. The particulars of the blade, together with the parent and the modified composite layup at the impact region and the modeling details are explained in Section 2 followed by a detailed discussion on the damage models in Section 3. Finally, results and discussions followed by conclusions are presented in Section 4 and 5 of this paper respectively.

2. Impact scenario and numerical modeling strategy

The present work considers the contact scenario when the leading edge of the lifted blade (near the yoke region) impacts the tower during lifting which can occur owing to wave induced motion especially highly sensitive roll motion. The numerical model for this work is based on the DTU 10 MW reference blade model and will be referred as 'base model' or 'parent model' in the remaining paper.

2.1. Contact scenario and contact region

The contact scenario along with the contact region of the blade are very important parameters to be considered in a contact/impact analysis of the blade during installation. In principle, the contact scenario depends upon the type of lifting method considered (Figure 3).

Type of Lifting method	Contact Region
a) Lifting of blade (Zero degree pitch angle)	Leading edge, trailing edge
b) Lifting of blade (Ninety degree pitch angle)	Pressure side, suction side

Figure 3. Illustration of type of lifting method and possible contact regions [42]

The often-used lifting method considered in the practice is the lifting of the blade either with a zero degree-pitch angle (horizontal lifting) or with a ninety degree-pitch angle (vertical lifting) (Figure 3) [29]. Horizontal lifting can cause the leading edge or the trailing edge side of the blade to impact the tower. On the other hand, the vertical lifting of the blade can cause the pressure or suction side of the blade vulnerable (Figure 3). Also, each scenario can have different contact regions and the criticality of the damage will vary as different sections of the blade are optimized with different composite layup. This paper investigates the scenario when the leading-edge side of the blade hits the tower during lifting operation under zero pitch angle (horizontal lifting) at a region ('A') quite close to the yolk region of the lift ($0.44 < r/R < 0.48$) with two different impact velocity considered: 0.1 m/s and 0.5 m/s (Figure 6-7).

2.2. Composite layup at the impact region

The base model utilized in this work is a DTU 10 MW blade model made of GFRP plies with balsa as core material and is 86.4 m (R) long with 5.4 m root diameter [25, 31]. The outer surface of the blade model except for the shear web was used as the shell reference surface to take into advantage the smoothness property [30] as well as to aid in the contact formulation as the impacts occur between the exterior surfaces of blade and the tower. The structural design perspective of the blade is based on a conventional approach using a load carrying box girder with two shear webs along with a third shear web closer to the trailing edge of the blade [31].

As per DTU parent model, the whole blade was partitioned into 11 regions circumferentially and 100 regions radially for defining composite layup. However, the main motive of the DTU 10 MW blade model was to check the global strength of the blade under global aerodynamic loads which is not sensitive to details of the layup definition and thus the stacking sequence based on multidirectional ply formulation was considered along with the properties derived based on Classical Laminate Theory [31] [32]. The layup considered was based on triaxial, biaxial and uniaxial nomenclature. The layup for the contact region of the blade ('A') considered in this paper based on this multidirectional nomenclature is presented in Figure 4. A triaxial ply in the layup is considered as a ply with [+45/-45/0] degree properties

with 35%, 35% and 30 % contribution respectively. Similarly, a biaxial ply was considered as ply with [+45/-45] degree properties with 50-50 % contribution and a uniaxial ply was considered as the ply with [0/90] degree ply properties with 95% and 5% contribution respectively.

The same composite layup based on the above nomenclature representing ply, with equivalent properties of individual plies, cannot be used for the study of impact analysis on the blade at the impact region. This is due to the fact that the nature of impact is very much sensitive to the layup and it is not possible then to explicitly say which layer is most critical to damage. A typical offshore wind blade utilizes individual ply stacked with +45, -45 and 0-degree angle with each orientation contributing to cater specific loading condition. 0° ply is for the bending stiffness whereas +45 and -45 ply are used to cater for torsional and buckling resistance [9, 16, 33]. Moreover, it has been found that the delamination arising at the interface of the ply cause sub-laminate buckling and can be very critical [11, 22, 23, 26, 27] which in principle cannot be captured by multidirectional stacking sequence. Thus, to explicitly say which ply through the thickness will be more critical would require a layup in a unidirectional nomenclature representing individual ply with their specific orientation.

Thus, the composite layup for the impact region of the blade was modified and defined (Figure 5) in the terms of individual plies layup orientation keeping the basic parameters like thickness of the region (34.6 mm), mass (42.37 tons) and COG of the blade (26.2 m from the blade root) constant. Further, eigenvalue analysis for the whole blade model along with the impact analysis with the tower gave consistent results for both parent and modified layup. The material properties were derived from the DTU 10 MW database as well as from [11, 22, 23, 26] and are listed in Table I of section III.

2.3. Numerical modelling and assumptions

The numerical modelling of the laminates and composites for the finite element analysis very much depends upon the choice of element which is determined by the kinematic assumption enforced [34] for a particular type of element based on the composite shell theory. The choice of element for modelling the composite blade shell for the impact analysis in this study was considered as general purpose thick shell S4R element (Figure 7). S4R thick shell element is a 4-node element with finite strain and is suitable for large strain analysis. Further, the S4R element is enforced by first order shear deformation theory (FSDT) also called as Mindlin shear flexible theory and estimates transverse shear stresses using a shear correction factor and is well suited to model thick laminates or materials with low shear modulus as is the case with the composite materials. For Mindlin shear flexible theory, straight lines normal to the mid plane remain straight but not necessarily normal after deformation and thus considers interlaminar shear strains and was found suitable to model the blade. However, the use of shell elements for the blade could only capture intralaminar failure mode in the blade and could not analyze delamination between the interfaces of the ply which could be critical for the blade under impact.

However, the delamination can be qualitatively predicted as the matrix cracking in the ply could further lead to delamination. Moreover, to explicitly understand the progressive damage of the delamination, use of cohesive elements or fracture mechanics approach is required and then the blade must be modelled with solid continuum elements which makes the analysis very computationally expensive. However, the scope of this paper is to investigate the failure modes using the DTU 10 MW blade model which is based on shell element formulation. For simplicity, the core material in the form of balsa was considered to be part of the layup stacking sequence itself (Ply 5, Figure 8). The outer layer of the blade shell is taken as the reference shell surface. This allows contact of the blade outer shell with the tower which is physically true. Moreover, adhesive material along the trailing edge was modelled with standard hexahedral continuum solid element with eight nodes and reduced integrations scheme (C3D8R) which were surface to surface tie constrained (Figure 7) with the upper and lower aerodynamic shell. Moreover, adhesive connections along the spar-web were modelled with a simple edge-to-edge connection. The tower considered in this numerical study has a diameter 5 m with height 110m and was modelled as a discrete rigid body with (R3D4) element (Figure 7) and with fixed encastre boundary condition. The blade was given initial velocity in the x-direction (V_x) with no velocity in other two direction ($V_y=V_z=0$). The study does not include the numerical modelling of wire or yolk of the crane

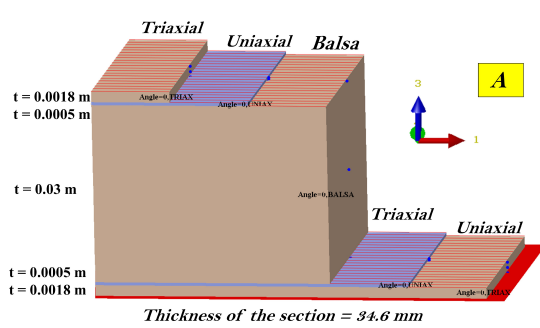


Figure 4. Composite Layup at the contact region (Parent DTU definition)

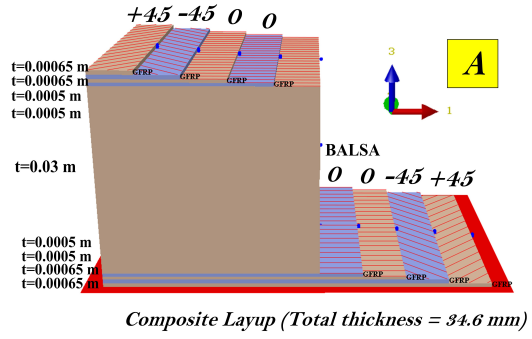


Figure 5. Composite Layup at the contact region 'A' (Modified layup at contact region 'A')

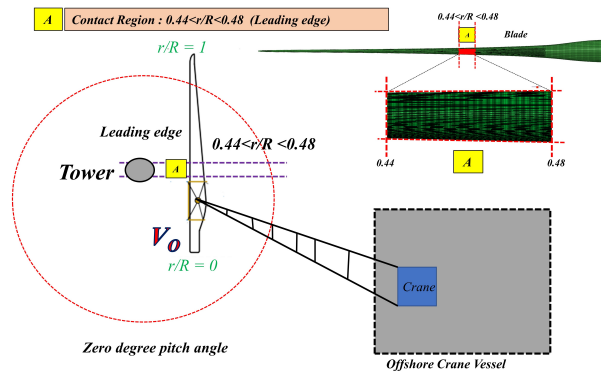


Figure 6. Bird view schematic representation of contact scenario and impact region of the blade marked with 'A' ($0.44 < r/R < 0.48$)

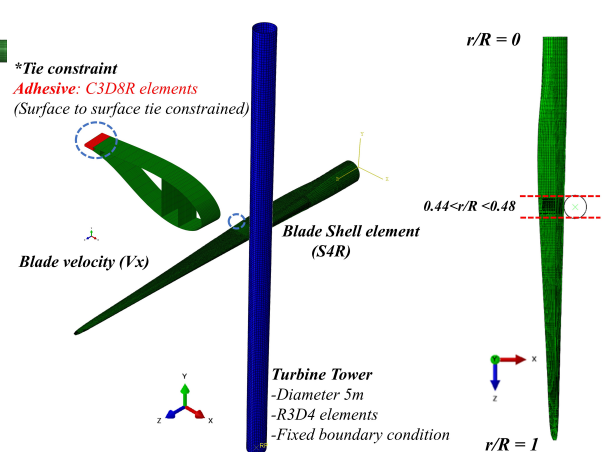


Figure 7. Numerical modelling detail for the blade and turbine tower

used for the lift and neglects the effect of gravity in the finite element study.

The contact between the blade reference surface and the tower outer surface was modelled using the general contact algorithm available in ABAQUS Explicit. The Penalty enforcement algorithm with a friction coefficient of 0.3 along with hard contact pressure over closure interaction behavior was defined. There was no mass scaling considered in any part of the model in the explicit analysis. Each ply was defined with 3 section points. Figure 8 shows section point's nomenclature considered while defining composite layup and it can be seen that there were 27 section points in total considered throughout the thickness out of which all section points other than 13, 14 and 15 were reserved for the composite material. The section points 13, 14 and 15 (Ply-5) were saved for outputting results for the balsa material. The post processing of results at section points makes it possible to get information for the individual ply in the shell based design of laminate composite structure. Figure 9 shows the mesh convergence study performed on the blade to calibrate result which will be independent of the mesh density. For this purpose, the maximum stress at the impact region was plotted with varying element sizes at the contact region for a case having velocity of impact as 0.1 m/s. The contact region finally had a very refined area with element dimension of $48 \times 48 \text{ mm}^2$ (S4R) with other region having a coarse mesh size with elements varying from 50 mm to 0.2 m with total 87,456 elements chosen and the analysis takes almost about 26 hours to complete. This is owing to small stable time increment required by ABAQUS kernel to handle very small element size in contact.

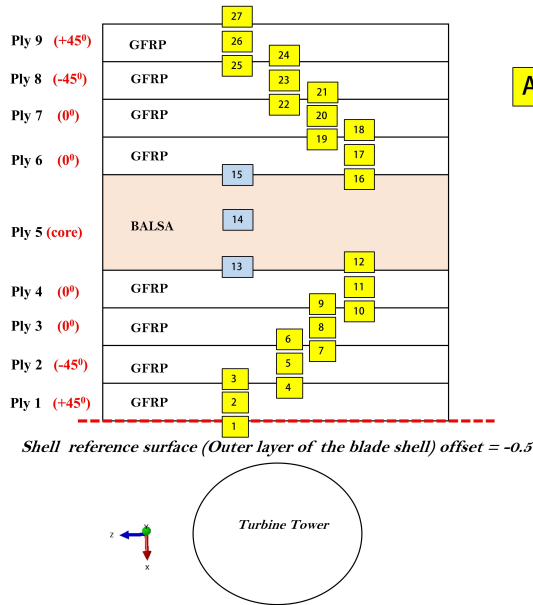


Figure 8. Composite layup with section points considered for each ply

3. Constitutive damage models for impact analysis on blade

The present paper utilizes damage models explicitly for intralaminar damage modes in the composite ply and damage in the balsa which is utilized as the core material in the blade. They are explained below briefly:

3.1. Intralaminar damage model for composite ply

The damage quantification and assessment of composites at the ply level can be evaluated based on stress or strain based failure criteria or by an appropriate polynomial based failure criteria like Tsai-Wu or Tsai-Hill or by continuum damage mechanics approach [9]. The analysis in this paper utilizes a very well known strength based failure criteria to evaluate the onset and propagation of fiber failure and matrix cracks also referred to as progressive damage model in ABAQUS and other finite element solvers [18, 19, 30, 35]. The intra-ply damage model in this paper is based on Hashin failure criteria along with the energy-based damage evolution law which is based on the work of [36, 37] and can effectively describe the post damage initiation behaviour. This progressive damage model can distinguish different stages of the composite under impact loading history.

The first phase is based on undamaged constitutive behaviour where the material is assumed to behave linearly elastic followed by a damage initiation point described by Hashin's failure criterion and post damage Initiation behaviour given by a damage evolution law [36, 37]. *Hashin and Rotem, et al. 1973* [38] proposed a failure criteria which was further modified by *Hashin 1980* [35] and it utilizes the effective stress space (σ') as the failure surface and can be used to predict four major damage mode in the composite laminates- matrix tension, matrix compression, fiber tension and fiber compression. The initiation criteria have the following general form [30, 35]:

1. Tensile fiber failure for $\sigma'_{11} \geq 0$

$$F_f^t = \left(\frac{\sigma'_{11}}{X^T} \right)^2 + \alpha \left(\frac{\tau'_{12}}{S^L} \right)^2 \quad (1)$$

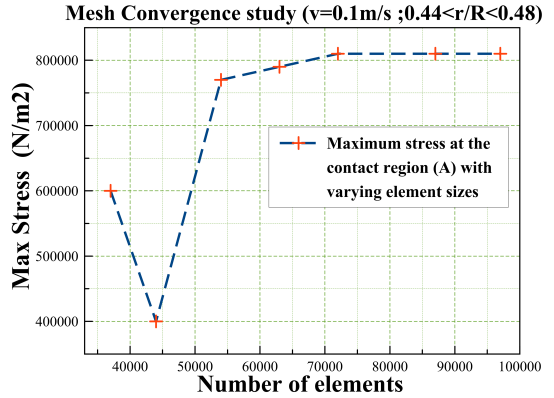


Figure 9. Mesh Convergence study for the global shell model

2. Compressive fiber failure for $\sigma'_{11} < 0$

$$F_f^c = \left(\frac{\sigma'_{11}}{X^c} \right)^2 \quad (2)$$

3. Tensile matrix failure for $\sigma'_{22} > 0$

$$F_m^t = \left(\frac{\sigma'_{22}}{Y^T} \right)^2 + \left(\frac{\tau'_{12}}{S^L} \right)^2 \quad (3)$$

4. Compressive matrix failure for $\sigma'_{22} < 0$

$$F_m^c = \left(\frac{\sigma'_{22}}{2S^T} \right)^2 + \left[\left(\frac{Y^c}{S^L} \right)^2 - 1 \right] \left(\frac{\sigma'_{22}}{Y^c} \right) + \left(\frac{\tau'_{12}}{S^L} \right)^2 \quad (4)$$

Where σ'_{ij} denote the effective stress tensor; X^T , X^c , Y^T and Y^c denotes the allowable tensile and compressive strength of unidirectional laminate in longitudinal and transverse direction respectively. Further, S_L , S_T denote the allowable in-plane and out of plane shear strength of the composites in their respective principal material directions [30]. Moreover, here α denotes the contribution of shear stress in the tensile fiber failure mode ($\alpha = 0$, in this study). Once the F_f^t , F_f^c , F_m^t or F_m^c reaches 1 for an integration point, it implies that the damage initiation criteria have been met for any of the four-possible mode of failure explained above. The results can be processed at all the section points through the thickness of the laminate defined for this study using output request HSNMTCRT, HSNFCCRT, HSNCMCCRT, and HSNFTCRT for tensile matrix failure, compressive fiber failure, compressive matrix failure and tensile fiber failure respectively except the section points 13, 14, 15 which are section points reserved for balsa material. Again, the energy based damage evolution is utilized, which is used to describe post damage initiation material behavior and calculate the stiffness of the damaged elements post damage initiation point by the relation given below:

$$\sigma = C_d \varepsilon \quad (5)$$

$$C_d = \frac{1}{D} \begin{bmatrix} (1-d_f)E_1 & (1-d_f)(1-d_m)\nu_{21}E_1 & 0 \\ (1-d_f)(1-d_m)\nu_{12}E_2 & (1-d_m)E_2 & 0 \\ 0 & 0 & (1-d_s)GD \end{bmatrix} \quad (6)$$

$$D = (1-d_f)(1-d_m)\nu_{12}\nu_{21} \quad (7)$$

$$d_f = \begin{cases} d_f^t & \text{if } \sigma'_{11} \geq 0 \\ d_f^c & \text{if } \sigma'_{11} < 0 \end{cases} \quad (8)$$

$$d_m = \begin{cases} d_m^t & \text{if } \sigma'_{22} \geq 0 \\ d_m^c & \text{if } \sigma'_{22} < 0 \end{cases} \quad (9)$$

$$d_s = (1 - d_f^t)(1 - d_m^c)(1 - d_m^t)(1 - d_m^c) \quad (10)$$

where C_d is the damaged material stiffness, d_f , d_m and d_s are damage variables estimated based on the evolution law given by stress-displacement relation with linear material softening [30] and represent the current damaged state for the fiber and matrix in different modes. This can be obtained by calling ABAQUS output card - DAMAGEMC (matrix compression), DAMAGEMT (matrix tension), DAMAGEFC (fiber compression), DAMAGESHR (shear) and DAMAGEFT (fiber tension) at the required section points of the ply.

3.2. Failure criteria considered for the core material :

The shear failure criteria for balsa material modelled as a part of shell composite layup in the blade section (Figure 9-13) is described with a very simple failure criterion and is based on von Mises stress criterion with equivalent plastic strain and considers the balsa as an elastic perfectly plastic material. The isotropic hardening is considered where the yield stress evolves as the plastic strain accumulates. Moreover, the damage model has been adopted and verified in the work by Nanami, et al 2012 [13, 14, 30]. Under this damage model, material yielding starts when von Mises stress reaches the allowable strength of balsa taken as 5.4MPa. This value is derived from [39]. Then, it is further assumed that failure occurs when the equivalent plastic strain corresponds to failure strain of balsa material which is taken as 0.8. The plasticity model is given by the following equation [30]:

$$\sigma_y = \sqrt{\sigma_{11}^2 + \sigma_{22}^2 - \sigma_{11}\sigma_{22} + 3\tau_{12}^2} \quad (11)$$

where σ_y is the von Mises stress and σ_{11} , σ_{22} , τ_{12} are components of in-plane effective stress vector, and accumulated plastic strain is given by

$$\varepsilon^{pl} = \varepsilon_0^{pl} + \int_0^t \sqrt{(2/3)\dot{\varepsilon}^{pl} : \dot{\varepsilon}^{pl}}, \quad (12)$$

where ε_0^{pl} is the initial equivalent plastic strain. The material properties for balsa as well as GFRP plies were obtained from [18, 19, 22, 23, 31] [31, 39-41] and are listed in Table 1.

Table 1. Material Properties implemented

S. No	Properties	Uniaxial	Biaxial	Triaxial	Balsa
1	ρ (Kg/m ³)	1915.5	1845.0	1683.0	110
2	E1 (GPa)	41.63	13.92	21.79	0.050
3	E2 (GPa)	14.93	13.92	14.67	0.050
4	E3 (GPa)	13.42	12.09	12.09	2.730
5	G12 (GPa)	5.047	11.50	9.413	0.0167
6	G23 = G13 (GPa)	5.0469	4.53	4.53	0.150
7	v_{12}	0.241	0.533	0.478	0.5
8	v_{23}	0.33	0.3329	0.3329	0.013
9	v_{13}	0.2675	0.275	0.275	0.013
10	X_T (MPa)	903.6	214.2	472.06	-
11	X_C (MPa)	660.1	184.8	324.16	5.4
12	$Y_T = Y_C$ (MPa)	42.1	184.8	127.12	-
13	$S_L = S_T$ (MPa)	58.65	143.9	99.25	-
14	G_{FT} (J/m ²)	1200	1200	1200	-
15	$G_{FC} = G_{MT} = G_{MC}$ (J/m ²)	4000	4000	4000	-

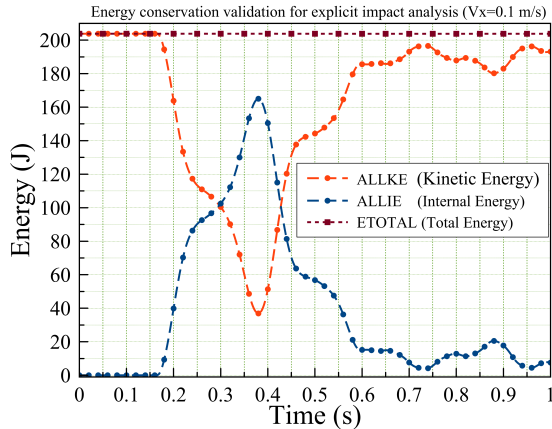


Figure 10. Variation of ALLKE, ALLIE and ETOTAL($V_x = 0.1 \text{ m/s}$ and $0.44 < r/R < 0.48$)

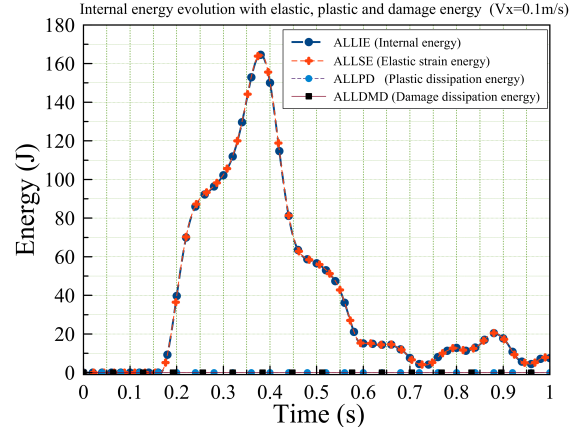


Figure 11. Evolution of ALLIE, ALLSE, ALLDMD and ALLPD ($V_x = 0.1 \text{ m/s}$ and $0.44 < r/R < 0.48$)

4. Results and discussion

This section deals with the results and discussion for damage analysis on the blade including assessment of damage initiation and damage evolution for the impact with the tower for two different impact velocity (a) 0.1 m/s (b) 0.5 m/s at the contact region ($0.44 < r/R < 0.48$) of the blade based on Hashin's intralaminar failure model for fiber and matrix damage for GFRP plies and von-Mises yield stress criteria with equivalent plastic strain indicator for balsa material in the shell layup. Also, the contact-force time history for the cases along with damage criterion for the most critical ply is reported and discussed in this section. Moreover, the discussion on the nature of evolution of different types of energy relevant for the impact scenario is made which in principle can also be qualitatively used to indicate the development of any damage.

Initial impact velocity 0.1 m/s :

The most important result for an impact analysis based on ABAQUS explicit algorithm is the check for the validity of energy conservation [30] and the nature of evolution of impact energy with time. This is required to confirm that the considered numerical model is fit to estimate damage assessment in the blade under impact scenario. Figure 10 shows the variation of kinetic energy (ALLKE), internal energy (ALLIE) and total energy (ETOTAL) involved in the simulation for the entire model and it can be seen that the ETOTAL is almost constant throughout the simulation and the sum of ALLIE and ALLKE corresponds to ETOTAL. Thus, the conservation of energy during the impact analysis on the blade is obtained. The simulation time to investigate this impact study was taken as 1 second with the blade coming in contact with the tower at 0.18s of the simulation time and at this time kinetic energy of the blade starts reducing with the development of internal energy in the blade. Now, this internal energy (ALLIE) in principle is utilized either as the elastic strain energy (ALLSE), damage dissipation energy (ALLDMD) or plastic deformation energy (ALLPD) based on the mechanics of the material under impact. The contact with the tower lasts till 0.58s of the simulation and the blade rebounds.

Figure 11 shows the variation of internal energy (ALLIE) with strain energy (ALLSE), plastic dissipation energy (ALLPD) and damage dissipation energy (ALLDMD) and it further confirms the validation of energy conservation during the impact analysis as the sum of ALLSE, ALLDMD, and ALLPD corresponds to ALLIE of the structure. Moreover, it was observed that ALLIE is almost similar to ALLSE throughout the simulation which implies that there is no noteworthy damage in the impact area. This is a very qualitative indicator of deciding whether there is damage in the material or not based

on energy results. The quantification of damage can further be done based on the damage model and failure criteria applied for specific materials which will be discussed later. Moreover, by analyzing the evolution of hourglass energy or the artificial energy (ALLAE), it was found that this energy was negligible. Thus, from all the above energy evolution results, it was confirmed that the considered numerical model can estimate evolution of damage in the blade during impact scenario.

Moreover, from the contact force time history (Figure 12), it can be seen that the curve is very smooth before and during the impact from 0.18 s to 0.21 s with maximum contact force reaching as around 33

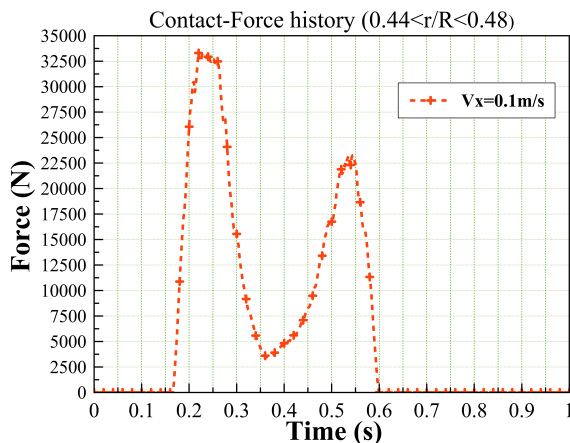


Figure 12. Contact force time history ($V_x = 0.1$ m/s and $0.44 < r/R < 0.48$)

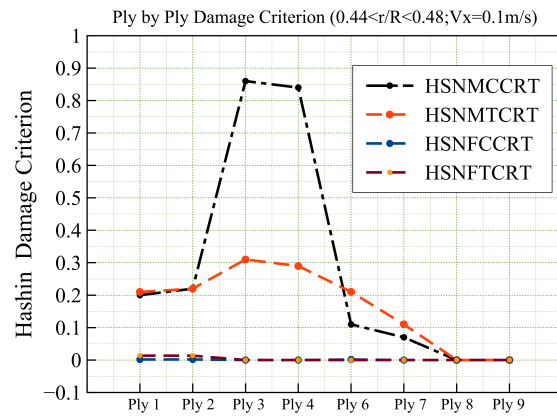


Figure 13. Ply by ply maximum Hashin damage criterion per element

kN at 0.21 s. After that, the contact-force curve displays a small vibration followed by decline and incline of contact area of the blade from 0.28 s to 0.34 s respectively (decline and incline of contact force). This is in-line with the observed edge wise vibration of the blade, together with a fluttering motion in the blade tip relative to the other region of the blade. This is due to the eccentricity of the contact region and a relatively lighter and tapered section of the blade towards the tip of the blade. The contact with the blade further lasts till 0.58 s and finally the blade rebounds. Further as per the implemented damage model, it was seen that none of the ply in the layup has damage criterion equal to one (Figures 13, 14), meaning that the damage initiation criteria was not met and thus there was no intralaminar damage initiation.

The maximum Hashin criterion was 0.83 in matrix compression damage mode (*HSNMCCRT*). Moreover, since there were three section points reserved for each ply during the preprocessing set up (except section points 13,14,15), it was possible to output the Hashin damage criterion at specific section points for each ply. This can help in identifying which ply through the thickness of the laminate is critical and prone to failure initiation. Moreover, for the cases, where there is actual damage achieved (Hashin failure criterion >1), it is also possible to quantify which ply is damaged (Figure 18(a)). However, for this case since the Hashin criterion was not met, no damage is initiated in any mode of failure. However, it is still possible to compare which ply has the highest damage criterion. Figure 13 presents the Hashin criterion developed at each ply level and it can be seen that Ply 3 and Ply 4 has the highest Hashin damage criterion more than 0.8 for the damage in matrix compression. None of the ply had Hashin damage criterion more than 0.1 for damage mode in fiber tension (*HSNFTCRT*) or compression (*HSNFCCRT*). Again, for the shell section points (13, 14, and 15) reserved for Ply no 5 for the balsa material, it was possible to check the highest von Mises stress or any plastic strain developed. However, it was found that the maximum stress levels (0.6-1.8 MPa) observed were quite lower than the allowable stress level of balsa which is taken as 5.4 MPa and it was further seen that there was no plastic strain developed in the balsa as it has not reached the yield strength (the output card PEEQ was unchecked). Moreover, adhesive elements around the trailing edge and the composite elements along the spar flange

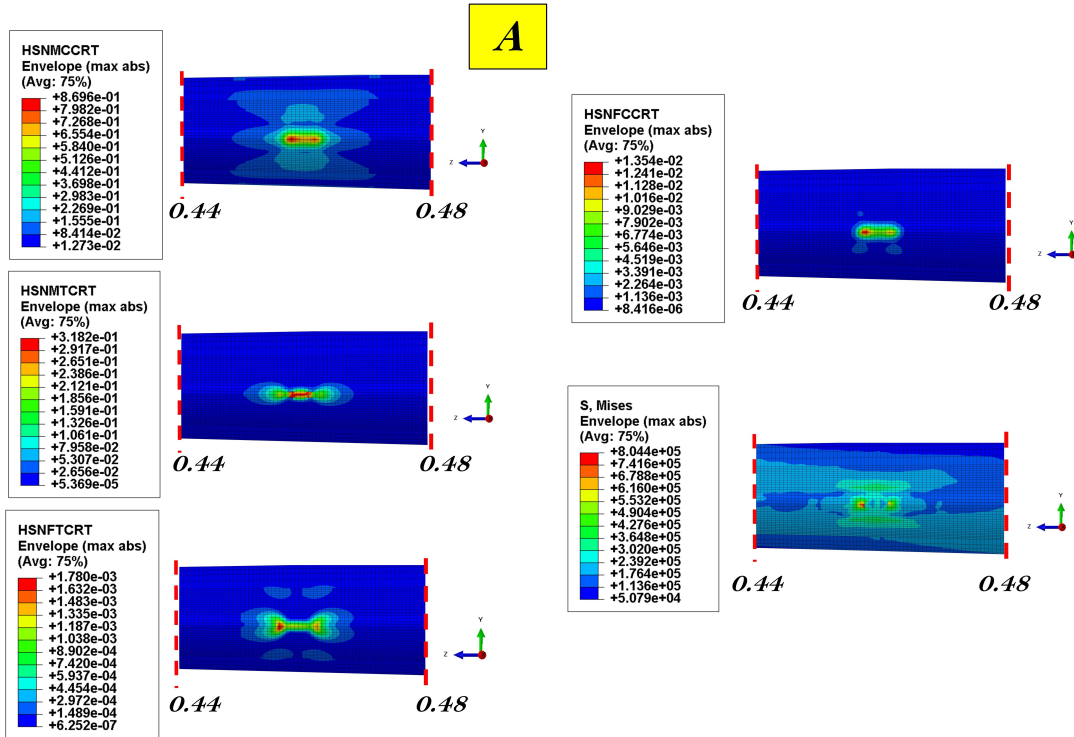


Figure 14. Hashin damage criterion for composite ply and von Mises stresses in Balsa ($V_x = 0.1 \text{ m/s}$)

and shear web connection had very low stress levels which further can imply qualitatively that these regions were safe during the impact.

Initial impact velocity 0.5 m/s:

The validation of energy conservation was very well observed for ETOTAL as well as ALLIE for this case when the blade impacts the tower at the initial velocity of 0.5 m/s, and hence the numerical model considered can be used to estimate damage evolution in the blade (Figure 15). However, in this case ALLSE is similar to the ALLIE only until 0.061 s of the total simulation time and can be seen that at this time ALLDMD appears and the damage initiation in the blade has started. Moreover, there was a very small development of ALLPD (Figure 15) in the numerical model which implies qualitatively that the balsa material would have developed a very small plastic strain and the stress levels at the section points (13, 14, 15) would have exceeded allowable stress value. The clear picture of this will be explained later when the damage is explained with regard to the damage models implemented.

Also, the blade comes in contact with the tower at 0.05 s. Figure 16 shows the contact force time history along with the evolution of ALLDMD where it can be seen that the nature of contact force curve with the first contact force peak follows the development of damage energy (only the first impact at the first contact force peak induces the damage and not the second peak, Figure 16). Once the maximum contact force of 163 kN along with maximum damage energy is reached, there is a rapid decrease in the force peak curve which implies damage state representing failure mode in the impact region. Again, this is just a qualitative indication of impact induce damage.

From the damage model implemented for the composite material, it was seen that the blade at the impact region has developed Hashin damage criterion equal to one in matrix compression and matrix tension failure mode (Figure. 18(e)) which implies the initiation of damage. Once, the criterion was met, the damage evolution law implemented would determine the final damaged state of the composite ply at the

impact region. It was found that post damage initiation, the final damaged state for the composite ply was checked for shear damage variable (DAMAGESHR), matrix tensile damage (DAMAGEMT) variable and matrix compression damage variable (DAMAGEMC) which implies that the composite plies had failed in shear, matrix compression and matrix tension failure modes.

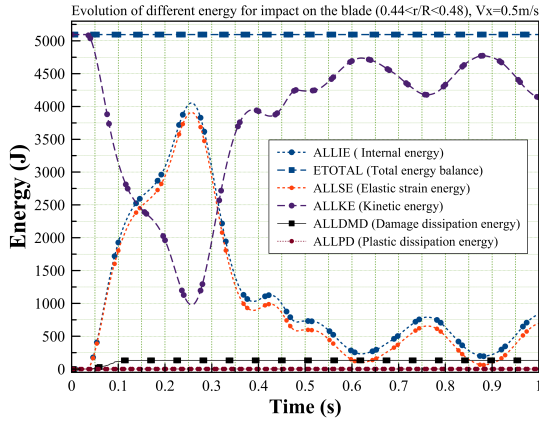


Figure 15. Evolution of various energy for the impact analysis ($V_x = 0.5$ m/s)

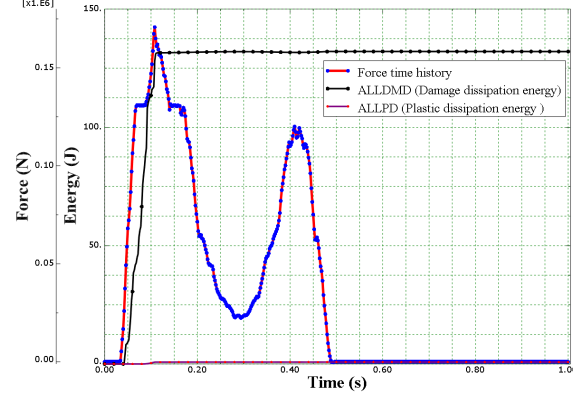


Figure 16. Contact force time history v/s ALLDMD ($V_x = 0.5$ m/s)

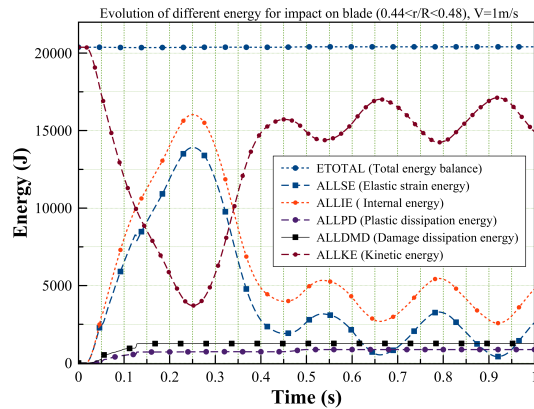


Figure 17. Contact force time history v/s ALLDMD ($V_x = 0.5$ m/s)

Figure. 18 (a) shows the envelope (max) for these variables as well as for the respective plies at the middle most section point which shows the maximum damages occurring in the impact area (ply wise) in different damage modes. It can be seen that the maximum damage occurs at the top most plies quite close to the impact region and they lie above the sandwich core balsa. However, Ply 6 which lies below the core, had some damage in matrix compression and shear. Moreover, different plies had different damage area given the fact the impact region had a curvature. The stress level and plastic strain output at the section points reserved for balsa material (13, 14 and 15) showed that there was development of plastic strain (Figure.18 (d)). However, it was well below the allowable plastic strain. Moreover, it can also be qualitatively argued that since Ply 1, Ply 2 and Ply 3 had developed matrix cracks, they have a high chance of developing delamination between them as it has been reported in the literature that matrix crack could lead to delamination in the ply with fibers of different orientations. The solid adhesive elements near the trailing edge had very low and acceptable stress level developed. However, some region far from the impact and along the spar flange and shear web connection developed considerable high stresses as seen from Figure. 18(c) and could failure of adhesive connections along the interface. This observation also develops the understanding that it is quite possible to see the effect of the impact

or damage area, quite far from the contact region and thus for higher velocity impacts, in order to see all possible damages and failure modes, the whole blade model must be studied in the analysis and suitable failure criteria must be implemented. Also, since the spar cap region did not have balsa material in the layup definition, it could cause the failure of adhesive connection by causing the failure of adherend itself. However, this is just a qualitative inference. In order to quantitatively analyze the failure of adhesive material, it would require a proper numerical modelling technique using fracture mechanics approach such as VCCT (Virtual Crack Closure technique) or by CZM (Cohesive Zone Modelling) approach. Such an analysis to utilize the cohesive elements at the interface of the spar flange and shear web region would come at a high computation cost and would require an efficient numerical modelling strategy and modification/adjustment on the available DTU 10 MW blade which is primarily based on shell element formulation.

From the energy evolution history for a case with impact velocity 1 m/s (Figure 17), it was observed that the damage energy and plastic deformation energy increases further rapidly. This significant increase in ALLPD also implies development of further damage to the core in the sandwich structure and it would require modifications/adjustments to the existing DTU 10 MW numerical blade model to capture other detailed failure mode under impact study. These modifications would also demand dedicated experiments/numerical study to an extent to validate blade behavior under impact evaluated with a numerical solver. This is planned to be addressed in the future research work.

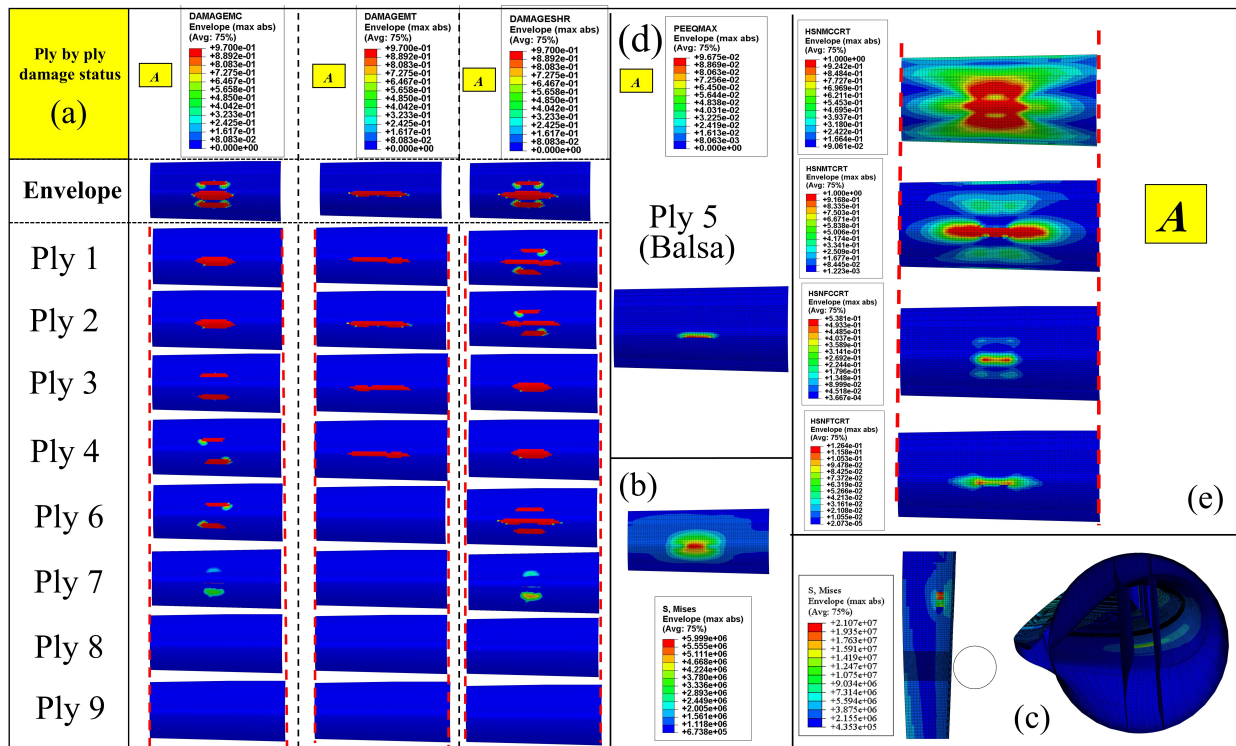


Figure 18. (a) Damage state of the composite ply ($t = 1\text{s}$) (b) Stress level developed in balsa (c) Stress level at spar flange and shear web region of the blade (d) Plastic strain developed (PEEQ) in balsa, Ply-5 (e) Hashin damage criterion developed at the impact region ($V_x = 0.5 \text{ m/s}; 0.44 < r/R < 0.48$)

5. Conclusions

In this investigation, the numerical simulation of impact analysis of the wind turbine blade with the tower during installation was performed using advanced capability of finite element study in ABAQUS explicit environment. The emphasis was on the progressive damage modelling on the available DTU 10

MW wind turbine composite blade model based on shell element formulation under a scenario when the leading edge of the blade hits the tower at the contact region ($0.44 < r/R < 0.48$). The whole purpose of such an analysis to estimate allowable sea state based on explicit structural response method was briefly mentioned. The details for the numerical modelling were described. Finally, the impact analysis was performed for two different velocity of impact- 0.1 m/s, 0.5 m/s. The impact energy varies with the square of velocity and thus it was found that for the case of 0.1 m/s, there was no damage in the blade and all the kinetic energy in the blade transferred to the internal energy was lost by the motion of the blade tip and excessive vibration at the contact region. However, for the case of 0.5 m/s, significant damage was observed in the impact region (A) of the blade and damaged state was quantified at the ply level. It was also found that it is even possible to get damage in the composite plies on the opposite side of the impacted surface. It can also be concluded that the damage threshold energy (DTE) would lie somewhere in between the impact energy for 0.1 m/s and 0.5 m/s. The stress levels along the spar flange and shear web connection far from the impact region experiences high stresses which implies the requirement of the whole blade for the numerical analysis with appropriate modelling technique required and cannot just be studied on the local area of the blade. The extent of damage is considerable under such scenario and thus in order to evaluate allowable damage, which allows installing the blade with some level of damage would require strength analysis on the damaged blade. Overall, computationally to further study and extract other possible failure modes like delamination in the ply and the failure of adhesive connection, some modifications are required on the available DTU 10 MW blade numerical model especially for relatively high velocity of impact. This will be addressed in future research. However, still for low velocity impact, the current model gives good notion of energy evolution and damage modes relevant for blade under impact especially intra-ply failure modes.

Acknowledgement

This work was made possible through the financial support from the Norwegian Research Council under Centre for Marine Operations in Virtual Environments (SFI MOVE), NFR project no. 237929. The authors would also like to thank DTU for making the blade numerical model available in public domain.

References

- [1] Rodrigues S, Restrepo C, Kontos E, Pinto RT, Bauer P 2015 Trends of offshore wind projects. *Renewable and Sustainable Energy Reviews*. 2015; **49** :pp 1114-35.
- [2] Li L, Gao Z, Moan T 2015. Comparative Study of Lifting Operations of Offshore Wind Turbine Monopile and Jacket Substructures Considering Vessel Shielding Effects. *The Twenty-fifth International Ocean and Polar Engineering Conference*; 2015: International Society of Offshore and Polar Engineers.
- [3] Gao Z, Wilson Guachamin Acero LL, Zhao Y, Li C, Moan T. 2016 Numerical simulation of marine operations and prediction of operability using response-based criteria with an application to installation of offshore wind turbine support structures. *Marine Operations Specialty Symposium (MOSS 2016)*.
- [4] Tegen S, Hand M, Maples B, Lantz E, Schwabe P, Smith A. 2012 *Cost of Wind Energy Review*. National Renewable Energy Laboratory (NREL), Golden, CO.; 2012.
- [5] Acero WG, Li L, Gao Z, Moan T. 2016 Methodology for assessment of the operational limits and operability of marine operations. *Ocean Engineering*. 2016; **125** :pp 308-27.
- [6] Acero WG, Gao Z, Moan T. 2017 Methodology for assessment of the allowable sea states during installation of an offshore wind turbine transition piece structure onto a monopile foundation. *Journal of Offshore Mechanics and Arctic Engineering* 2017.
- [7] Li L, Gao Z, Moan T. Operability analysis of monopile lowering operation using different numerical approaches. *International Journal of Offshore and Polar Engineering*. 2016; **26(02)** :pp 88-99.
- [8] Kim H, DeFrancisci G, Halpin J. *Impact Damage of Composite Structures*. Long-Term Durability of Polymeric Matrix Composites. 2012; **3**: pp (143-180)

- [9] Abrate S. *Impact on composite structures*: Cambridge university press; 2005.
- [10] El-Reedy MA. *Offshore structures: design, construction and maintenance*: Gulf Professional Publishing; 2012.
- [11] Haselbach PU, Bitsche R, Branner K. The effect of delaminations on local buckling in wind turbine blades. *Renewable Energy*. 2016; **85** :pp 295-305.
- [12] Feng D. *Simulation of low-velocity impact damage in sandwich composites*: Universita'degli Studi di Cagliari; (PhD Thesis), 2014.
- [13] Nanami N, Ochoa O. Bird Impact Study of a Preloaded Composite Wind Turbine Blade. Paper Presented at the *The 19th International Conference on Composite Materials, Montreal, Canada*.
- [14] Nanami N, Ochoa O. Damage Assessment of a Large-Scale Hybrid Composite Wind Turbine Blade. *Journal of Mechanical Engineering and Automation*. 2016; **6(5)** :pp 117-27.
- [15] Agrawal S, Singh KK, Sarkar P. Impact damage on fibre-reinforced polymer matrix composite—a review. *Journal of Composite Materials*. 2014; **48(3)** :pp 317-32
- [16] Abrate S, Ferrero J, Navarro P. Cohesive zone models and impact damage predictions for composite structures. *Meccanica*. 2015; **50(10)** : pp 2587-620.
- [17] Bernal AN. *Simulation of the low-velocity impact behavior of glass reinforced composite pipes*: The Petroleum Institute (United Arab Emirates); 2015.
- [18] Perillo G, Jørgensen J. Numerical/Experimental Study of the Impact and Compression after Impact on GFRP Composite for Wind/Marine Applications. *Procedia Engineering*. 2016; **167** :pp 129-37.
- [19] Perillo G, Vedivik N, Echtermeyer A. Numerical and experimental investigation of impact on filament wound glass reinforced epoxy pipe. *Journal of Composite Materials*. 2015; **49(6)** :pp 723-38.
- [20] Reiner J, Torres JP, Veidt M, Heitzmann M. Experimental and numerical analysis of drop-weight low-velocity impact tests on hybrid titanium composite laminates. *Journal of Composite Materials*. 2016; **50(26)** :pp 3605-17.
- [21] Skaar MW. *Modeling and Testing of Impact Damage in Composite PressureVessels*: NTNU; (Master thesis), 2015.
- [22] Haselbach PU, Branner K. Initiation of trailing edge failure in full-scale wind turbine blade test. *Engineering Fracture Mechanics*. 2016; **162** :pp 136-54.
- [23] Haselbach PU, Eder MA, Belloni F. A comprehensive investigation of trailing edge damage in a wind turbine rotor blade. *Wind Energy*. 2016; **19(10)** : pp 1871-88.
- [24] McGugan M, Pereira G, Sørensen BF, Toftegaard H, Branner K. Damage tolerance and structural monitoring for wind turbine blades. *Phil Trans R Soc A*. 2015; **373(2035)** :2014.
- [25] Jensen FM. *Ultimate Strength of a Large Wind turbine Blade (PhD Thesis)*: Risø National Laboratory, Technical University of Denmark; 2008.
- [26] Haselbach PU. *Ultimate Strength of Wind Turbine Blades under Multiaxial Loading*: DTU Wind Energy; (PhD Thesis), 2015
- [27] Toft HS, Branner K, Berring P, Sørensen JD. Defect distribution and reliability assessment of wind turbine blades. *Engineering Structures*. 2011; **33(1)** :pp 171-80.
- [28] Minakuchi S, Okabe Y, Mizutani T, Takeda N. Barely visible impact damage detection for composite sandwich structures by optical-fiber-based distributed strain measurement. *Smart Materials and Structures*. 2009; **18(8)** :085018.
- [29] Zhao Y Cheng Z, Sandvikd PC, Gao Z, Moan T. An integrated dynamic analysis method for simulating installation of a single blade for offshore wind turbines (In press) *Ocean Engineering* 2017.
- [30] ABAQUS V. 6.14 Documentation. Dassault Systemes Simulia Corporation. 2014.
- [31] Bak C, Zahle F, Bitsche R, Kim T, Yde A, Henriksen LC, et al., editors. *The DTU 10-MW reference wind turbine*. Danish Wind Power Research 2013.

- [32] Reddy JN. *Mechanics of laminated composite plates and shells: theory and analysis* : CRC press; 2004.
- [33] Cox K, Echtermeyer A. Structural design and analysis of a 10MW wind turbine blade. *Energy Procedia*. 2012; **24** :pp 194-201.
- [34] Barbero EJ. Finite element analysis of composite materials using AbaqusTM: *CRC press*; 2013.
- [35] Hashin Z. Fatigue failure criteria for unidirectional fiber composites. ASME, Transactions, *Journal of Applied Mechanics*. 1981; **48** :pp 846-52.
- [36] Camanho PP, Davila C, De Moura M. Numerical simulation of mixed-mode progressive delamination in composite materials. *Journal of composite materials*. 2003; **37(16)** :1415-38.
- [37] Camanho PP, Dávila CG. *Mixed-mode decohesion finite elements for the simulation of delamination in composite materials*. (NASA) 2002.
- [38] Hashin Z, Rotem A. A fatigue failure criterion for fiber reinforced materials. *Journal of composite materials*. 1973; **7(4)** :pp 448-64.
- [39] Vural M, Ravichandran G. Microstructural aspects and modeling of failure in naturally occurring porous composites. *Mechanics of Materials*. 2003; **35(3)** :pp 523-36.
- [40] Nanami N. *Structural and Damage Assessment of Multi-Section Modular Hybrid Composite Wind Turbine Blade* 2014 (PhD Thesis), Texas A&M University
- [41] Weijermars W. *Mechanical behaviour of composite sandwich panels in bending after impact*. 2016 (Master thesis), University of Twente., Enschede, Netherlands
- [42] Aymerich F. Composite materials for wind turbine blades: issues and challenges, SYSWIND Summer school-July 2012-University of Patras, Italy (Schematic of the cross-section of the blade with different parts).